# Accurate Simulations of the Vapor−Liquid Equilibrium of Important Organic Solvents and Other Diatomics

**S. Lago,* B. Garzón,† S. Calero, and C. Vega**

*Departamento de Química Física, Facultad de Ciencias Químicas, Universidad Complutense, 28040 Madrid, Spain*

*Received: March 13, 1997; In Final Form: June 2, 1997*[⊗]

The vapor−liquid equilibria of 20 substances, most of them widely used as organic solvents, were obtained by means of a Gibbs ensemble Monte Carlo method. All these substances can be represented by linear or angular models with only two bonds. The intermolecular interaction was described by a Kihara potential and, where appropriate, an additional multipolar potential using meaningful microscopic parameters. The results agree excellently with experiment even for ranges of hundreds of kelvin when potential parameters are obtained only from fitting two critical constants. The largest discrepancies are observed for liquids capable of forming hydrogen bonds, especially alcohols, but even in these cases agreement is very fair for temperature−density equilibrium bells. Agreement is also very good for vapor pressure up to close to critical pressure, namely 60−80 bar in all cases. The worst agreement is again observed for hydrogen-bonding liquids. Vaporization enthalpies were also calculated for some substances. In this case agreement was only fair but also over a large range of temperatures. Finally, parameters commonly used in chemical engineering, such as the acentric factor and solubility factor, which enable prediction of the mutual solubilities of some hundreds of mixtures, were calculated. Some of these mixtures are not yet apparently measured in spite of their possible industrial interest.

## I. Introduction

Vapor−liquid equilibrium (VLE) is one of the most important properties in chemical engineering,[1] and a large number of empirical equations of state (EOS) have been proposed[2] to calculate it for pure liquids as well as for mixtures. Usually, empirical EOS have a restricted application range and involve parameters depending on macroscopic properties such as temperature, density, or pressure, thus making their microscopic physical meaning questionable. In spite of these shortcomings, empirical EOS are friendly to use and are broadly used. On the other hand, approximations physically better founded on a molecular vision, such as perturbation theories,[3,4] are more difficult to use, even in their simplest variants.[5] Furthermore, perturbation results can confidently be used because they use parameters independent of macroscopic variables. Although perturbation theories do not yield better results than empirical EOS in narrow pressure and temperature ranges, they do over large ranges.[3,5] Here, we should also refer to an important recent theory for associating liquids, hydrogen-bonded liquids, and polymers: the SAFT theory[6−8] based on previous ideas of Wertheim,[9−14] which accounts for the wealth of behavior of associating liquids and their mixtures[15,16] while maintaining only a slight semiempirical basis. An intermediate point of view between pure empiricism and the more complicated theories can be reached by using simulation results. In Monte Carlo (MC) or Molecular Dynamics (MD) simulation, parameters have the same straightforward physical meaning as in theories but mathematical instruments are conceptually as simple as Newton equations in molecular dynamics or the generation of random numbers in Monte Carlo.[17] In the last few years, we have indeed performed extensive computations on molecular models[18] mimicking linear or quasi-linear or simple nonlinear molecules, including in some cases dipole[19] or quadrupole[20] interactions. These models correspond to a large number of organic solvents widely used in the chemical industry. So, the main goal of this paper is to show how the models can give quantitative results from first principles only. The results are accurate enough over a very large range of temperature and density, corresponding to nearly all states from the triple to the critical point on the VLE curve. The method used here is the Monte Carlo simulation in the Gibbs ensemble, known in short as GEMC, originally proposed by Panagiotopoulos.[21] GEMC allows for the simultaneous determination of coexistence densities and vapor pressure at a fixed temperature in only one simulation run. The intermolecular potential was a simple Kihara potential,[22] formally equal to the well-known Lennard-Jones potential, for the dispersive interactions, plus an additional multipole interaction in some cases. This multipole interaction was always taken as a point dipole or quadrupole placed on the molecule center in the case of linear models or on the angle apex in the case of nonlinear models. Simulated fluids were divided into six classes according to their constitutive molecules in the following way:

(a) "spherical" molecules containing dipoles: methanol, methylamine, methyl chloride, methyl fluoride, and methylene fluoride.

(b) "linear" molecules without multipoles: oxygen, nitrogen, chlorine and ethane.

(c) "linear" molecules with quadrupole: perfluorethylene and perfluorethane.

(d) "linear" molecules with dipole: ethanol, ethylamine, and 1,1-difluorethane.

(e) "linear" molecules with dipole and quadrupole: acetonitrile, fluorethylene, and 1,1-difluorethylene.

(f) "angular" molecules: isopropylamine, propane, and perfluoropropane.

The results obtained here include the VLE curve, the EOS on this curve, and vaporization enthalpy. We show that agreement with experiment is, in general, excellent except for liquids forming hydrogen bonds, especially the above alcohols. We also obtained important technical parameters such as the acentric factor and solubility parameter, evaluated at 293.15 K for most of these liquids. We are restricted in this paper to

* Author to whom correspondence should be addressed.

† Present address: Dpto. Ciencias Básicas (Química Física), Fac. CC. Experimentales y Técnicas, Universidad San Pablo CEU, Urb. Montepríncipe, Boadilla del Monte, 28668 Madrid, Spain.

⊗ Abstract published in *Advance ACS Abstracts,* July 15, 1997.

S1089-5647(97)00933-4 CCC: $14.00 

solvents with a relatively simple molecular structure and simple intermolecular potential, but simulations using the same GEMC technique and more complicated intermolecular potentials, including in some cases molecular flexibility, have been reported for alkanes[23,24] and alkanols,[25,26] completing the picture of VLE for a large number of organic liquids.

Industry is interested not only in pure liquids, even though they may be as important as those shown here, but also very often in binary or more complex mixtures. Simulations in mixtures are possible but very inefficient if the composition of the mixture is not previously given. So, in this paper we have simply opted for a discussion of binary mixtures in terms of solubility parameters, though aware of all the limitations of this point of view. Simulation again offers an important advantage over direct experiment or purely empirical EOS and opens the way to obtaining solubility parameters easily at any density and temperature from the simulated VLE curve, giving more confidence to the predictions.

Bearing all these ideas in mind, the schedule of this paper is very simple. Section II presents the essential details of the simulation methods as well as the necessary equations to relate experimental and simulation variables. Section III shows our results for VLE and vaporization enthalpy from simulation, compared with experiment. This section is divided into six subsections according to the classification of liquids given above. Section IV shows the more important technical parameters, the acentric factor and solubility parameter, their relation to microscopic parameters, and predictions for binary mixtures. A short discussion closes the paper.

## II. Simulation Conditions and Relation to Experiment

Simulations were performed in the Gibbs ensemble using the method proposed by Panagiotopoulos.[21] This method enables the determination of coexistence densities at a given temperature in only one run. Details of the simulations are identical to those described in other papers,[18−20] and we only give here some additional details. The simulated liquids are thought to be composed of spherical, linear, or angular molecules interacting through dispersive forces plus, where appropriate, multipole forces including dipole−dipole, quadrupole−quadrupole, and dipole−quadrupole according to the kind of substances. Dispersive interactions and short range repulsions are described by a Kihara intermolecular potential[22] whose functional form is the same as the well-known Lennard-Jones potential:

$$u_{12}^{K} = 4\epsilon[(\sigma/\rho)^{12} - (\sigma/\rho)^{6}] \qquad (1)$$

Now, $\rho$ is the shortest distance between the molecular cores and, thus, depends on the vector joining the molecular centers as well as intermolecular mutual orientations. The molecular core is simply a dot for almost spherical molecules (class a), a rod for the linear ones (classes b, c, d, and e), and a pair of rods joined by an extreme and forming an angle close to the experimental bond angle for the angular ones (class f). Models and reference frame are shown in Figure 1 for linear and angular cores. Computation of $\rho$ is not trivial but we have developed several efficient algorithms in the last few years.[27−29] These algorithms allow for the computation of $\rho$ several millions of times per second even using a PC. Parameters for the molecules are obtained by fitting the density and critical temperature of the models to experiment and are shown in the first few rows of Tables 1−6. Using only this information and a wise choice of elongation, based on experimental bond distances and multipole moments, a large number of simulations were carried out for thermodynamic states lying between about 0.7 and 0.95 times the critical temperatures. Indeed, it was necessary to simulate only a relatively small number of models of elongations

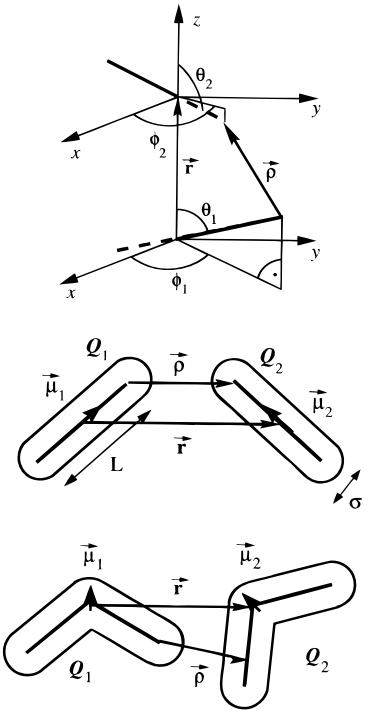


**Figure 1.** Molecular models for (pseudo)linear and angular molecules. The reference frame used in simulations is also shown.

**TABLE 1: Model Parameters and Estimated Thermodynamic Properties for Spherical Dipolar Fluids**

| | $CH_3OH$ | $CH_3NH_2$ | $CH_3Cl$ | $CH_3F$ | $CH_2F_2$ |
|---|---|---|---|---|---|
| $T_c$ (K) | 518.64 | 430.7 | 416.25 | 317.69 | 351.6 |
| $n_c$ (mol·L$^{-1}$) | 8.49 | 8.33 | 7.19 | 8.82 | 8.27 |
| $L^*$ | 0 | 0 | 0 | 0 | 0 |
| $\mu^{*2}$ | 4 | 2 | 2 | 4 | 4 |
| $\epsilon/k$ (K) | 247.57 | 266.76 | 257.81 | 153.42 | 169.8 |
| $\sigma$ (Å) | 3.84 | 3.93 | 4.12 | 3.79 | 3.88 |
| $P_c$ (bar) | | | | | |
| exp | 80.92 | 76.14 | 66.79 | 58.77 | 58.3 |
| MC | 80.1 | 83.7 | 69.8 | 51.7 | 53.5 |
| $\mu$ (D) | | | | | |
| exp | 1.7 | 1.3 | 1.94 | 1.82 | 1.96 |
| MC | 2.78 | 2.99 | 2.23 | 2.14 | 2.34 |
| $T_b$ (K) | | | | | |
| exp | 338 | 267 | 249 | 195 | 221 |
| MC | 307 | 237 | 233 | 198 | 219 |
| $Z_c$ | | | | | |
| exp | 0.22 | 0.21 | 0.27 | 0.25 | 0.24 |
| MC | 0.22 | 0.28 | 0.28 | 0.22 | 0.22 |
| $\omega$ | | | | | |
| exp | 0.556 | 0.292 | 0.153 | 0.187 | 0.271 |
| MC | 0.22 | 0.12 | 0.12 | 0.22 | 0.22 |
| $\delta$ | | | | | |
| exp | 14.5 | 11.2 | 9.3 | 9.2 | |
| MC | 13.0 | 9.4 | 8.3 | 5.9 | 7.5 |

between $L^* = 0$. and $L^* = 0.8$ and different integer values of $\mu^{*2}$ and/or $Q^{*2}$ to obtain good agreement with experiment. These simulations were enough to build all the complete VLE curves. Values of $L^*$ and $\mu^{*2}$ are shown in the corresponding lines in Tables 1−4. Simulations closer to the critical point are not possible, and we have calculated this point using the rectilinear diameter law and a critical exponent equal to $^1/_3$, close to the universal critical exponent as determined by experiment or from renormalization group theory.[30] The critical point is probably the most difficult point to fit the parameters, but this procedure enables the parameters to be obtained in a totally unambiguous way. Easier choices[3,31] are possible, but in this case the parameters depend slightly on the particular thermodynamic states used to fit them. Moreover, we have found[19,20] that reduced critical temperatures are independent of elongation for the Kihara potential when a reduced dipole/quadrupole density is properly defined and we have made use of this fact here.

**TABLE 2: Model Parameters and Estimated Thermodynamic Properties for Nonpolar Linear Fluids**

| | $O_2$ | $N_2$ | $Cl_2$ | $CH_3CH_3$ | $CH_3CH_3$ |
|---|---|---|---|---|---|
| $T_c$ (K) | 154.58 | 126.2 | 416.95 | 305.34 | 305.34 |
| $n_c$ (mol·L$^{-1}$) | 13.63 | 11.21 | 8.13 | 6.88 | 6.88 |
| $L^*$ | 0.6 | 0.3 | 0.3 | 0.3 | 0.6 |
| $\epsilon$/k (K) | 138.7 | 113.24 | 416.75 | 273.98 | 305.2 |
| $\sigma$ (Å) | 3.00 | 3.20 | 3.21 | 3.77 | 3.39 |
| $P_{c\ (bar)}$ | | | | | |
| exp | 50.43 | 34 | 75 | 42.48 | 42.48 |
| MC | 51.9 | 34.8 | 86.1 | 51.7 | 53.3 |
| $T_{b\ (K)}$ | | | | | |
| exp | 90 | 77 | 239 | 185 | 185 |
| MC | 89 | 76 | 242 | 176 | 186 |
| $Z_c$ | | | | | |
| exp | 0.29 | 0.29 | 0.29 | 0.29 | 0.29 |
| MC | 0.30 | 0.30 | 0.30 | 0.30 | 0.30 |
| $\omega$ | | | | | |
| exp | 0.025 | 0.039 | 0.09 | 0.099 | 0.099 |
| MC | 0.15 | 0.0 | 0.0 | 0.0 | 0.15 |
| $\delta$ | | | | | |
| exp | | | | | 6.0 |
| MC | | | 11.7 | 3.3 | 4.0 |

**TABLE 3: Model Parameters and Estimated Thermodynamic Properties for Quadrupolar Linear Fluids**

| | $CF_2$═$CF_2$ | $CF_3CF_3$ |
|---|---|---|
| $T_c$ (K) | 306.5 | 293 |
| $n_c$ (mol·L$^{-1}$) | 5.8 | 4.51 |
| $L^*$ | 0.8 | 0.8 |
| $Q^{*2}$ | 3 | 3 |
| $\epsilon/k$ (K) | 264.87 | 253.2 |
| $\sigma$ (Å) | 3.62 | 3.83 |
| $P_c$ (bar) | | |
| exp | 39.4 | 30.4 |
| MC | 41.6 | 30.5 |
| $Q$ (B) | | |
| exp | | |
| MC | 7.7 | 9.3 |
| $T_b$ (K) | | |
| exp | 198 | 195 |
| MC | 195 | 192 |
| $Z_c$ | | |
| exp | 0.28 | 0.28 |
| MC | 0.28 | 0.28 |
| $\omega$ | | |
| exp | 0.223 | |
| MC | 0.22 | 0.22 |
| $\delta$ | | |
| exp | | |
| MC | 3.9 | |

**TABLE 4: Model Parameters and Estimated Thermodynamic Properties for Linear Dipolar Fluids**

| | $CH_3CH_2OH$ | $CH_3CH_2NH_2$ | $CHF_2CH_3$ |
|---|---|---|---|
| $T_c$ (K) | 513.9 | 456.2 | 386.4 |
| $n_c$ (mol·L$^{-1}$) | 5.99 | 5.52 | 5.57 |
| $L^*$ | 0.6 | 0.6 | 0.6 |
| $\mu^{*2}$ | 4 | 4 | 4 |
| $\epsilon/k$ (K) | 419.4 | 372.3 | 315.3 |
| $\sigma$ (Å) | 4.15 | 3.65 | 3.64 |
| $P_c$ (bar) | | | |
| exp | 61.4 | 56.3 | 45.2 |
| MC | 60.5 | 49.5 | 42.3 |
| $\mu$ (D) | | | |
| exp | 1.7 | 1.3 | 2.3 |
| MC | 3.2 | 3.2 | 2.9 |
| $T_b$ (K) | | | |
| exp | 351 | 290 | 248 |
| MC | 317 | 287 | 249 |
| $Z_c$ | | | |
| exp | 0.24 | 0.27 | 0.25 |
| MC | 0.24 | 0.24 | 0.24 |
| $\omega$ | | | |
| exp | 0.644 | 0.289 | 0.256 |
| MC | 0.23 | 0.23 | 0.23 |
| $\delta$ | | | |
| exp | 10.0 | 10.0 | 8.9 |
| MC | 9.6 | 9.8 | 7.2 |

The equations used in this work were

$$(n_l^* + n_g^*)/2 = a + bT^* \tag{2}$$

**TABLE 5: Model Parameters and Estimated Thermodynamic Properties for Linear Dipolar and Quadrupolar Fluids**

| | $CH_3CN$ | $CH_2$═$CHF$ | $CH_2$═$CF_2$ |
|---|---|---|---|
| $T_c$ (K) | 547.85 | 328 | 303 |
| $n_c$ (mol·L$^{-1}$) | 5.77 | 6.94 | 6.46 |
| $L^*$ | 0.8 | 0.6 | 0.6 |
| $\mu^{*2}$ | 8 | 1.5 | 1.5 |
| $Q^{*2}$ | 1 | 1 | 1 |
| $\epsilon/k$ (K) | 357.42 | 287 | 265 |
| $\sigma$ (Å) | 3.318 | 3.4 | 3.5 |
| $P_c$ (bar) | | | |
| exp | 48.3 | 52.3 | 44.6 |
| MC | 56.5 | 50.8 | 43.7 |
| $\mu$ (D) | | | |
| exp | 3.92 | 1.4 | 1.4 |
| MC | 3.8 | 1.5 | 1.5 |
| $Q$ (B) | | | |
| exp | 1.8 | | |
| MC | 4.45 | 4.2 | 4.3 |
| $T_b$ (K) | | | |
| exp | 354.8 | 201 | 187 |
| MC | 367 | 202 | 190 |
| $Z_c$ | | | |
| exp | 0.253 | 0.28 | 0.27 |
| MC | 0.215 | 0.27 | 0.27 |
| $\omega$ | | | |
| exp | 0.327 | 0.157 | 0.14 |
| MC | | 0.16 | 0.16 |
| $\delta$ | | | |
| exp | 12.1 | | |
| MC | 12.5 | 5.7 | 4.3 |

**TABLE 6: Model Parameters and Estimated Thermodynamic Properties for Angular Fluids**

| | $CH_3CHNH_2CH_3$ | $CH_3CH_2CH_3$ | $CF_3CF_2CF_3$ |
|---|---|---|---|
| $T_c$ (K) | 472 | 369.85 | 345 |
| $n_c$ (mol·L$^{-1}$) | 4.52 | 5 | 3.34 |
| $L^*$ | 0.3 | 0.4123 | 0.4 |
| $\mu^{*2}$ | 1.9 | 0 | 2.5 |
| $Q^{*2}$ | 0.3 | 0 | 1.5 |
| $\epsilon/k$ (K) | 470 | 392.59 | 367 |
| $\sigma$ (Å) | 3.95 | 3.59 | 4.15 |
| $P_c$ (bar) | | | |
| exp | 45.4 | 42.5 | 26.8 |
| MC | 51.7 | 43.4 | 26.7 |
| $\mu$ (D) | | | |
| exp | | 0 | |
| MC | 2.8 | 0 | 3 |
| $Q$ (B) | | | |
| exp | | | |
| MC | | | |
| $T_b$ (K) | | | |
| exp | 305 | 231 | 236 |
| MC | 281 | 221 | 221 |
| $Z_c$ | | | |
| exp | 0.26 | 0.28 | 0.28 |
| MC | 0.29 | 0.28 | 0.29 |
| $\omega$ | | | |
| exp | 0.291 | 0.153 | 0.325 |
| MC | 0.07 | 0.05 | 0.09 |
| $\delta$ | | | |
| exp | | 6.4 | |
| MC | 7.4 | 5.8 | 4.2 |

$$n_l^* - n_g^* = c\left(1 - \frac{T}{T_c}\right)^{1/3} \tag{3}$$

Alternatively, eq 3 can be written as

$$(n_l^* - n_g^*)^3 = f - gT^* \tag{4}$$

Simulations were carried out using 512 particles enclosed in two boxes with 256 particles in each box. Initial molecular configurations were taken as corresponding to an α-$N_2$ lattice in each box for temperatures close to the critical one. The volumes of the boxes were calculated to approximately fit the experimental densities. For the initial configurations at lower temperatures, we took the final configurations from a previous simulation at the immediately higher temperature. Each GEMC

simulation run yields reduced values for gas and liquid densities $n_g^*$ and $n_l^*$, respectively, where $n^* = n\sigma^3$, and $n$ is the particle numerical density for any phase at the reduced vapor pressure $p^* = p\sigma^3/\epsilon$ and at a fixed reduced temperature $T^* = Tk_B/\epsilon$, where $k_B$ is Boltzmann's constant. The internal energies of liquid, $U_l^*$ , and gas, $U_g^*$, phases are also computed during the same run. These values are used to calculate vaporization enthalpy as

$$\Delta H_v^* = \Delta U^* + p^*\Delta V^* = \Delta H_v/(N\epsilon) \tag{5}$$

Vapor pressure was fitted to a Clausius−Clapeyron law:[32]

$$\ln p^* = d - (e/T^*) \tag{6}$$

The simulation fitting parameters can easily be associated with experimental parameters. So, reduced critical variables can be written as

$$T_c^* = f/g \tag{7}$$

$$n_c^* = a + bT_c^* \tag{8}$$

$$P_c^* = \exp\left(d - \frac{e}{T_c^*}\right) \tag{9}$$

because liquid and gas densities are the same at the critical point. The corresponding absolute values of these properties are now equated to the experimental points as

$$T_c^{GEMC} = T_c^*(\epsilon/k) = T_c^{exp} \tag{10}$$

$$n_c^{GEMC} = n_c^*/\sigma^3 = n_c^{exp} \tag{11}$$

and potential parameters can be obtained from

$$\epsilon/k(\mathrm{K}) = \frac{T_c^{exp}(\mathrm{K})}{T_c^*} \tag{12}$$

$$\sigma(\text{Å}) = \left[\frac{n_c^*\cdot 10000}{n_c^{exp}(\mathrm{mol/L})\cdot 6.023}\right]^{1/3} \tag{13}$$

Once $\sigma$ and $\epsilon$ are obtained, it is very easy to transform reduced to absolute values using the following equations

$$T(\mathrm{K}) = T^*(\epsilon/k) \tag{14}$$

$$n(\mathrm{mol/L}) = \frac{10000n^*}{6.023(\sigma(\text{Å}))^3} \tag{15}$$

$$\frac{\Delta H_v}{N}(\mathrm{J/mol}) = \Delta H_v^*\cdot(\epsilon/k)\cdot k\cdot N_A \tag{16}$$

$$P(\mathrm{bar}) = \frac{P^*\cdot(\epsilon/k)\cdot 138.05}{(\sigma(\text{Å}))^3} \tag{18}$$

$$L = L^*\cdot\sigma \tag{19}$$

$$\mu(\mathrm{D}) = [\mu^{*2}\cdot(\epsilon/k)\cdot 138.05 \times 10^{-4}\cdot(\sigma(\text{Å}))^3]^{1/2} \tag{20}$$

$$Q(\mathrm{B}) = [Q^{*2}\cdot(\epsilon/k)\cdot 138.05 \times 10^{-4}\cdot(\sigma(\text{Å}))^5]^{1/2} \tag{21}$$

where the reduced dipole and quadrupole moments are defined by

$$\mu^{*2} = \mu^2/(\epsilon\sigma^3) \tag{22}$$

$$Q^{*2} = Q^2/(\epsilon\sigma^5) \tag{23}$$

respectively. Debye (D) and buckingham (B) are the most commonly used practical units for dipole and quadrupole moments, and their equivalence to SI units is 1 D = 3.33564 $\times 10^{-30}$ C·m and 1 B = 1 D × 1 Å. The angstrom is also not a SI unit, and its well-known equivalence is 1 Å = $10^{-10}$ m. Detailed results for each substance will be considered in the next section.

## III. Thermodynamic Properties

**(a) Dipolar Spherical Molecules.** Substances in this group were modeled by a spherical core plus a point dipole. This is equivalent to a Stockmayer potential whose properties are well characterized using integral equations.[33] Again, integral equations are not too easy to solve for these systems, and simulations are also valuable. Most of these substances correspond to methyl derivatives and molecular parameters are shown in Table 1 and the VLE curve in Figure 2. Hereafter, simulation results will be presented as continuous lines and experimental results with different symbols. Agreement is excellent in the density−temperature plot for halomethanes where experimental data are available[34,35] for more than 200 K. Agreement is slightly worse for methylamine[36] where the experimental range is also more narrow and still worse for methanol.[34] These observations are also valid for the pressure−temperature plot drawn according to the Clausius−Clapeyron law in Figure 2b where $p_0$ = 100 000 Pa as in all those considered below.

Vaporization enthalpy was also computed, and the results are shown in Figure 2c. Agreement between experiment and simulation remains very good for non-hydrogen-bond-forming substances, and it would be possible to obtain reliable results if necessary for heat capacity on the VLE curve and for a broad temperature range. In particular, our results for methyl fluoride lie between two series of experimental data that show some discrepancy. However, agreement is poor for methanol at low temperatures, and we are not aware of experimental data for methylamine.

A very remarkable feature shown in Table 1 is that fitting dipole moments are consistently larger than experimental moments. This difference should be attributed to the induced dipole moment caused by the neighboring molecules on a particular molecule in the liquid bulk. The induced dipole moment should be proportional to the polarizability, and a recent perturbation theory[37] explicitly accounts for this variation for a Stockmayer potential. The same trends are observed for more complicated liquids of classes d, e, and f with practically no exception, and we come back to this point below.

Some other properties are also shown in Table 1 and a similar discussion can be established on them.

**(b) "Linear" Molecules with No Multipole.** The molecular parameters and relevant thermodynamic and structural parameters for these kinds of liquids are shown in Table 2. Most, but not all of them, correspond to diatomics, and their VLE curves are shown in Figure 3. In this case, agreement with experiment[38−41] is excellent for a very broad range of temperatures. It is extremely remarkable that ethane can be represented accurately by a simple linear model even at temperatures close to the critical point. So, we can expect that dispersion interactions can be modeled nicely by a single rod not only for strict diatomics but also for pseudiatomics, namely those possessing a linear structure when the hydrogen atoms are depleted. Indeed, we found two parameter sets, with different elongations, that represent ethane equally well. Figure 3 shows the results corresponding to both parameter sets in Table 2, but they are indistinguishable at the scale of the figure. We found a similar result for acetonitrile,[42] and we shall come back to this point below. It is also remarkable that VLE curves for

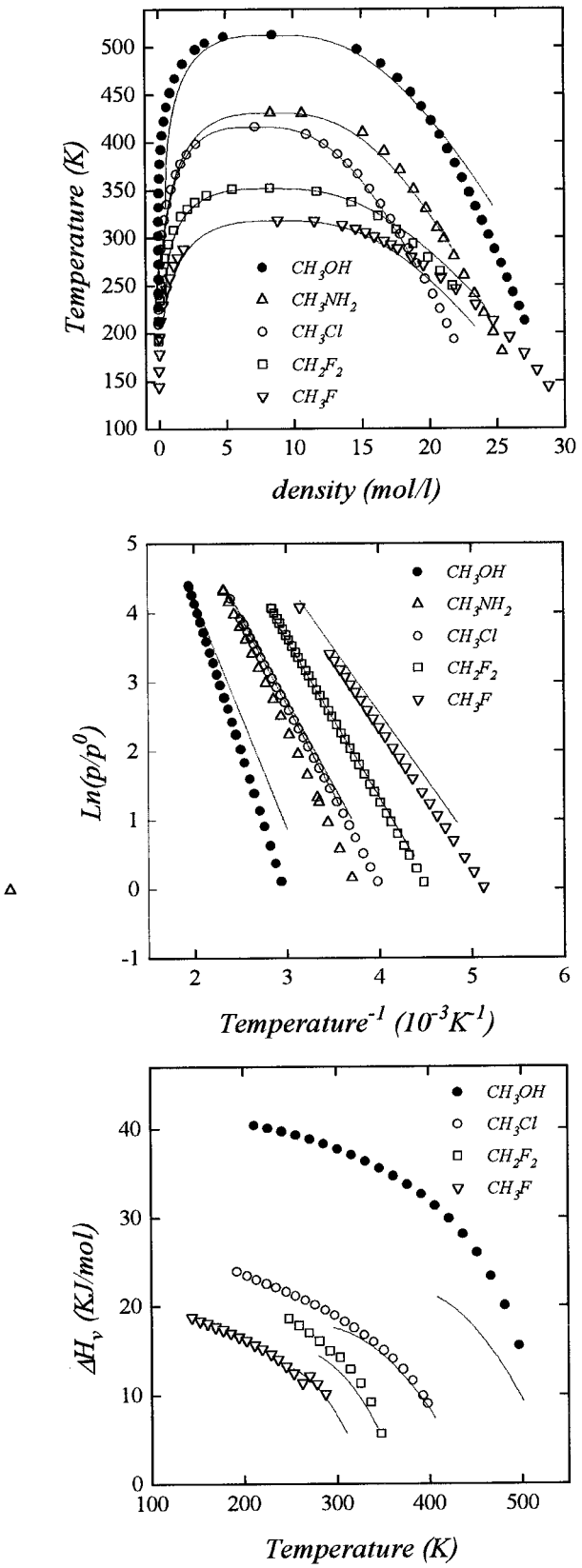


**Figure 2.** Polar spherical molecules: (a) vapor−liquid coexistence curve; (b) vapor pressures; (c) vaporization enthalpy. Symbols correspond to experiments, and continuous curves indicate the results of simulations. Experimental sources are ref 34 for halocompounds and methanol and also ref 35 for difluormethane and ref 36 for methylamine.

simpler fluids are very flat because of the relatively small liquid range of these substances when expressed in kelvin. However, agreement is also excellent in these cases.

**(c) Quadrupolar "Linear" Molecules.** VLE curves for these systems are shown in Figure 4, while molecular parameters

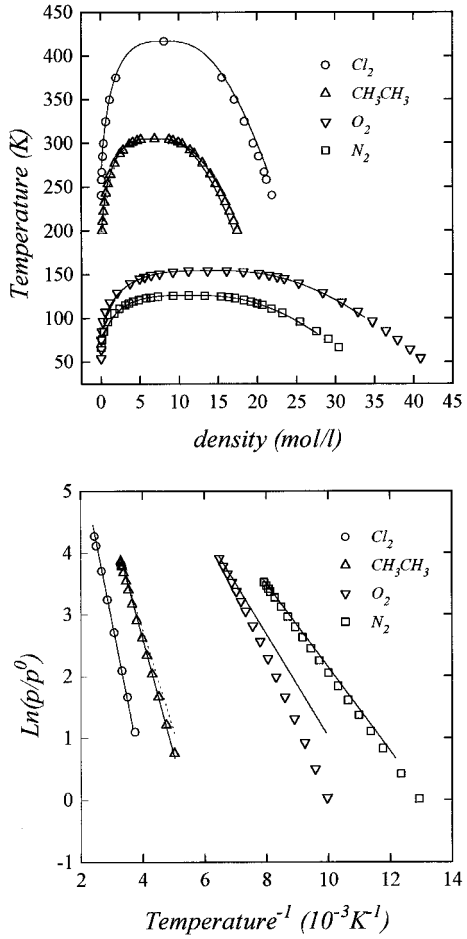


**Figure 3.** As in Figure 2 but for nonpolar linear molecules. Experimental sources are refs 38, 39, 40, and 41 for chlorine, oxygen, nitrogen, and ethane, respectively.

and chosen thermodynamic properties are also shown in Table 3. Agreement is again very good in the whole temperature range where experimental data are available.[34] No systematic deviation was observed for the most complicated molecular shape or for the presence of internal rotation in the case of perfluorethane. We previously studied this case for carbon dioxide, with excellent results,[20] and we can predict that a model of carbon dioxide without quadrupole would have a critical temperature 60 K lower than the quadrupole model of actual $CO_2$. We have shown that this behavior is general when reduced quadrupole density is properly defined. Therefore, similar conclusions may be established for the molecules in this group. In general, we can say that molecules in this group correspond to symmetric ethyl derivatives but with strong polar bonds, such as C−F.

**(d) Dipolar "Linear" Molecules.** Any system containing nonvanishing dipoles also has nonvanishing higher moments. This is a well-known fact. So, the molecules whose thermodynamic properties are shown in Table 4 have important dipole moments and certainly nonzero quadrupoles. However, thermodynamic properties are determined in these cases by the lowest multipole moment as in the above class, and we were able to find meaningful potential parameters, shown in Table 4, that show excellent agreement with experiment[34,36,43], as shown in Figure 5. As above, some important thermodynamic properties are also shown in Table 4. The worst agreement corresponds to ethanol[34] and, to a lesser extent, to ethylamine,[36] which are substances capable of forming hydrogen bonds, like those discussed in class a. However, we should point out that agreement is very good even for ethanol in a range of about 300 K in spite of all the difficulties described above. In general,

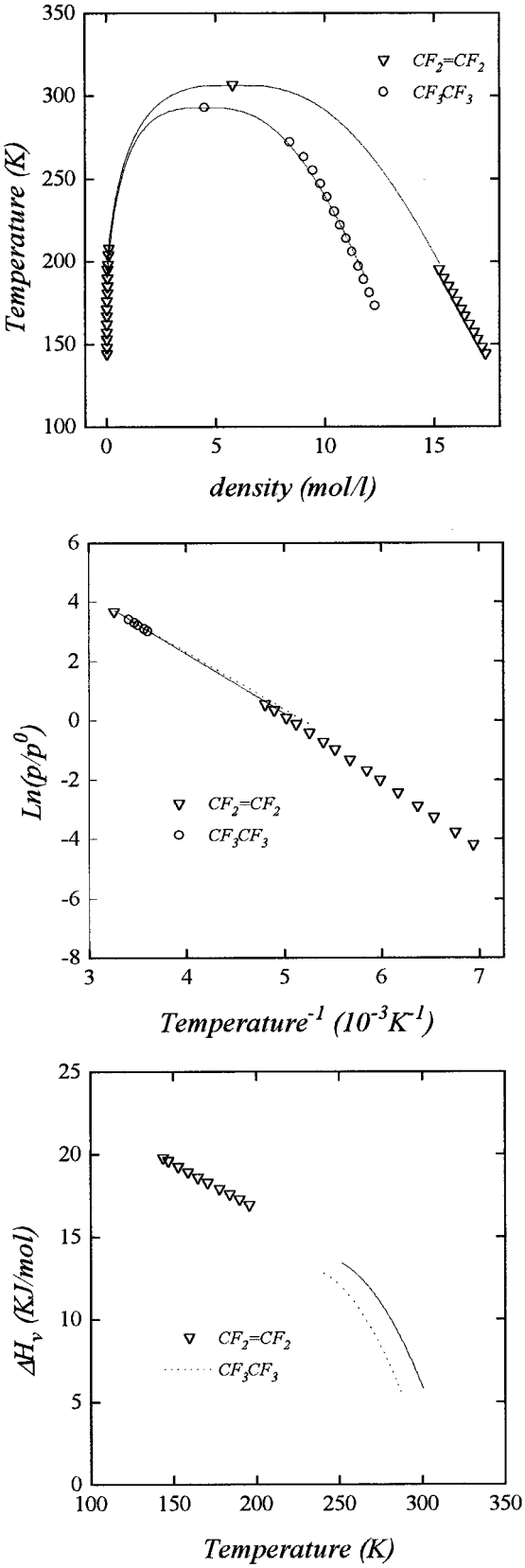


**Figure 4.** As in Figure 2 but for quadrupolar linear molecules. Experimental source is ref 34.

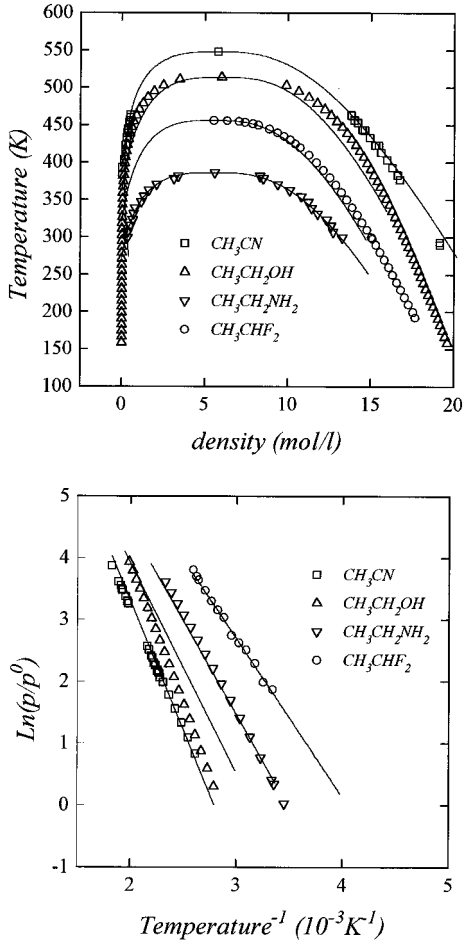


**Figure 5.** As in Figure 2 but for dipolar linear molecules. Experimental sources are refs 34 and 43 for difluoretane, ref 36 for ethylamine, ref 34 for ethanol, and ref 44 for acetonitrile.

we observe that the molecules belonging to this group correspond to ethyl derivatives containing one polar bond or two nonsymmetric polar bonds: C−O, C−N, and C−F in our case. However, the carbon skeleton and punctual dipoles suffice to give an accurate description of the VLE. We can see that simulated dipole is always larger than experimental dipole in a gaseous phase. As for class a, this difference can be attributed to the molecular polarizability, which does not explicitly appear in our formulation but induces some dipole moment. Similar behavior is observed for classes e and f.

**(e) "Linear" Molecules with Embedded Dipole and Quadrupole.** This class contains a series of molecules carrying a very high dipole moment and we failed to obtain fair agreement with experiment[34,44] even using very high dipoles with no physical meaning. In this case, we have to include a high dipole and a relatively high quadrupole to predict the VLE curve correctly as shown in Figure 6, except for acetonitrile, which is shown in Figure 5 for the sake of clarity. The molecule of trifluorethanol analyzed in a previous paper[19] would also belong to this class. Considering dipole−dipole, quadrupole−quadrupole, and dipole−quadrupole interactions, agreement is now very good for a range of more than 200 K. Furthermore, VLE is very well described for 1,1-difluorethylene in a very broad temperature range where experimental data are available for this substance. Experimental data for vaporization enthalpy are also available[34] over a large temperature range and agreement with simulation is also very good, especially for the range 240−280 K, perhaps the most important for this substance, since difluorethylene can be used as a refrigerant liquid. Results for acetonitrile require more detailed comment. In this case, we were able to find two different parameter sets that showed similar very good agreement with the experimental equilibrium curve and vapor pressure.[44] Nevertheless, these two models predict totally different dynamic properties, and this aspect is analyzed in depth elsewhere.[42] We observed that the molecules corresponding to this group are, in general, nonsymmetric compounds containing multiple bonds. The same remarks as

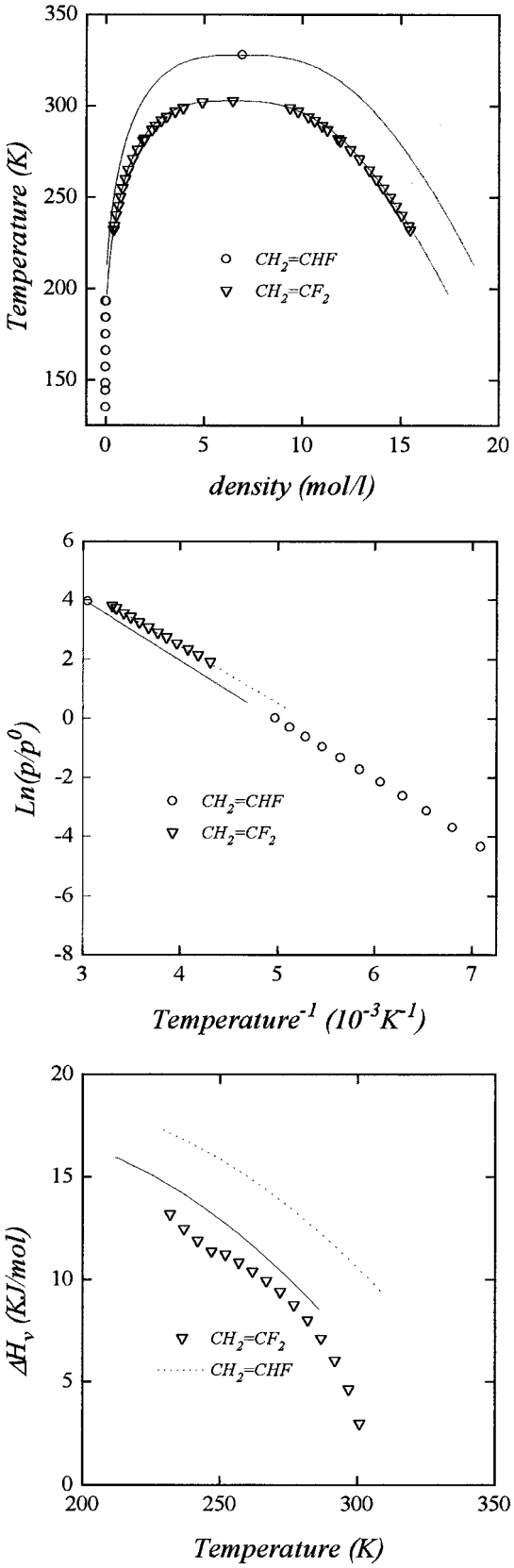


**Figure 6.** As in Figure 2 but for dipolar + quadrupolar linear molecules. Experimental source is ref 18.

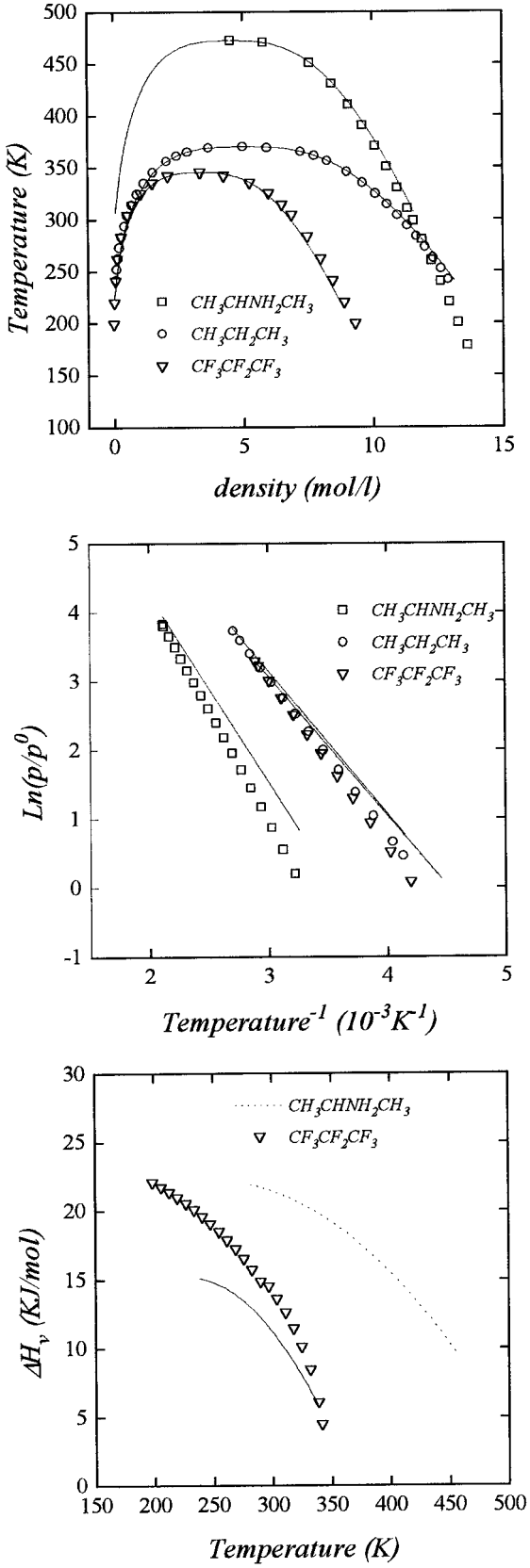


**Figure 7.** As in Figure 2 but for angular molecules. Experimental sources are ref 41 for propane, ref 34 for octafluorpropane, and ref 36 for isopropylamine.

those referring to the carbon skeleton for class e molecules also hold true here.

**(f) Angular Molecules.** These molecules have more complicated shapes than those considered up to now, but the choice of a reasonable model and GEMC simulation yield very good agreement with experiment as shown in Figure 7 for propane,[41] a molecule with negligible dipole moment, as well as perfluorpropane,[34] which carries a high dipole moment. Point dipole or quadrupole is placed on the apex of the angular model and the dipole vector is directed along the symmetry axis of the model. Good agreement for propane was also shown, and this is discussed elsewhere.[45] Results for vaporization enthalpy for perfluoropropane are also fair. Results for isopropylamine[36]

**TABLE 7: Predicted Miscibility at 293.15 K of Binary Mixtures of Molecules Considered in This Paper[a]**

| substance | 1 | 2 | 3 | 4 | 5 | 6 | 7 | 8 | 9 | 10 | 11 | 12 | 13 | 14 |
|---|---|---|---|---|---|---|---|---|---|---|---|---|---|---|
| 1. methanol | T | T | | | | | I | I | I | I | I | I | I | I |
| 2. acetonitrile | T | T | T | | | | I | I | I | I | I | I | I | I |
| 3. chlorine | | T | T | | | | | I | I | I | I | I | I | I |
| 4. ethylamine | | | | T | T | T | | | | | | | I | I |
| 5. ethanol | | | | T | T | T | | | | | | | I | I |
| 6. methylamine | | | | T | T | T | | | | | | | I | I |
| 7. methyl chloride | I | I | | | | | T | T | T | | | | I | I |
| 8. methylene fluoride | I | I | I | | | | T | T | T | T | | | | |
| 9. isopropylamine | I | I | I | | | | T | T | T | T | | | | |
| 10. 1,1-difluorethane | I | I | I | | | | | T | T | T | | | | |
| 11. propane | I | I | I | | | | | | | | T | T | | |
| 12. vinyl fluoride | I | I | I | I | | | | | | | T | T | | |
| 13. perfluorpropane | I | I | I | I | I | I | I | | | | | | T | T |
| 14. perfluorethylene | I | I | I | I | I | I | I | | | | | | T | T |

[a] T means total miscibility as predicted from solubility parameters. $\delta_J = \delta_I \pm 1$. I means total immiscibility taken as $|\delta_J - \delta_I| > 4$.

are also quite good but slightly worse. We cannot say in this case whether the deviations are due to dipole moments or to the presence of hydrogen bonds. Molecular parameters and thermodynamic properties are shown in Table 6. Obviously, the liquids corresponding to class f are more or less propyl or isopropyl derivatives. All these molecules are asymmetric tops with three different elements in the diagonal polarizability tensor, and conclusions on the relationship between the elements of this tensor and induced dipole moment would require more extensive simulations but, in general, they seem to follow the trends mentioned above for simpler dipolar molecules.

## IV. Chemical Engineering Parameters

Two of the most celebrated parameters used in chemical engineering are the acentric factor[46] defined as

$$\omega = \log_{10} (p/p_c)_{T=0.7T_c} - 1 \tag{24}$$

and the Hildebrand solubility parameter[47] defined as

$$\delta = ((\Delta H_V - RT)/V)^{1/2} \tag{25}$$

where $\Delta H_V$ is given in cal·mol$^{-1}$ (1 cal = 4.18 J) and $V$ is the molar volume of the liquid in cm$^3$ mol$^{-1}$. The acentric factor gives an idea of molecular deviations from sphericity due either to molecular shape or to anisotropic multipolar forces in some mixed way and is dimensionless. The solubility parameter is used in regular solution theory to predict important properties of mixtures, especially mutual liquid miscibility. Its units are (cal/cm$^3$)$^{1/2}$, which is often called H(ildebrand). The acentric factor is independent of temperature and values corresponding to the substance of this work are shown in Tables 1−6 for the different liquids. The acentric factor as obtained by simulation depends only on parameters $L^*$ and $\mu^{*2}$ (or $Q^{*2}$). The acentric factor can be measured only if the critical constants are known and is estimated from simulation with a large error. The solubility factor depends on temperature, and values at 293.15 K are also shown in the last row of Tables 1−6 for the substances in liquid state at this temperature. The solubility factor can be obtained from experiment at any temperature where $\Delta H_V$ and $V$ are available and can also be obtained accurately from simulations except in the vicinity of the critical point where $\Delta H_V = 0$ and any small error in $\Delta H_V$ is immediately reflected in $\delta$.

The solubility parameter seems to be more sensitive to molecular features than the acentric factor. Thus, class a liquids have very similar acentric factors when obtained by simulation and can be divided into two groups with $\omega \cong 0.12$ and $\omega \cong 0.22$, although all of them have a different $\delta$. Agreement between simulation and experiment is better for the $\delta$ parameter, and this agreement is quantitative except in the vicinity of the critical point, where small deviations in density or vaporization enthalpy have a greater influence. Moreover, we have shown[48] that consideration of a different dielectric constant to account for the reaction field (RF) surrounding a molecule has little or no influence on VLE, in general, and we systematically take $\epsilon_{RF} = \infty$. However, if we take the more realistic value given by a fitting from computer simulations[49] to $y = (4\pi n\mu^2)/(9k_BT)$, then $\delta = 14.4$ for methanol agrees excellently with experiment. For the rest of the molecules and states considered here, the exact value of $\epsilon_{RF}$ has a negligible influence, and even in this case, great uncertainties remain on this point due to the extrapolation procedure. Therefore, we used $\epsilon_{RF} = \infty$ for all the simulations reported here.

A similar discussion can be established for class b molecules, where chlorine and ethane have a very similar acentric factor but totally different solubility parameters. Apparently, the acentric factor shows mixed behavior due to the effect of the combination of shape and multipolar forces, which is extremely difficult to unravel. Agreement between simulated and experimental parameters is only qualitative in some cases, but both series of parameters show the same trends. The poor agreement for $\delta$ in the case of ethane must be attributed to its vicinity to the critical point.

Agreement is much better for classes c, d, and e, where agreement between experimental and simulated acentric factors is sometimes remarkable. In some cases, such as methanol, the relatively poor agreement is easily understood because our molecular parameters are fitted at the critical point and, as we pointed out above, the lowest temperature of our simulations is $T/T_C \cong 0.7$, just where the acentric factor is defined. Solubility parameters are not subject to this limitation and can be defined at any temperature, thus giving greater depth to the agreement.

A rule of thumb says that two liquids are totally miscible if their solubility parameters differ by a quantity less than 1. So, remembering that special care should be taken when applying this rule to mixtures containing amines or alcohols, we have drawn up Table 7, where the miscibility of a lot of important industrial mixtures is predicted. In this table we added an additional empirical rule, stating that liquids whose solubility parameters differ by more than 4 are totally immiscible. We restricted this table to the compounds where our predictions were in good agreement with experiment at 293.15 K. So, substances whose critical points are close to this temperature are not included. Substances were placed in Table 7 in order of decreasing solubility parameter, and a clear picture of groups of miscible substances is obtained. Moreover, there are in some cases clear chemical resemblances. So, in spite of its limitations, Table 7 provides a very useful guide to predicting the mutual miscibility of these liquids. This table strongly recalls the well-known table from the *Handbook of Chemistry and Physics*,[50] which quotes the paper by Drury,[51] and agreement can be

discussed case by case, with very fair overall agreement. For a given mixture we can say that the closer the experimental and simulated $\delta$ parameters, the more confidently Table 7 can be used. An interesting example is that afforded by acetonitrile, which is widely used as an eluent in column chromatography because of its immiscibility with many organic solvents, as predicted in Table 7. Furthermore, some of these binary mixtures, and especially ternary mixtures containing some of these components, do not seem to have been measured previously, and experimental data are still required,[52] which gives an idea of the relevance of this table.

## V. Short Conclusions

We have shown that GEMC simulations can accurately account for thermodynamic properties of pure organic solvents over ranges of some hundreds of kelvin. So, our results can confidently be used to interpolate in most experimental conditions on the VLE curve. The key to obtaining good results is to model the molecules with reasonable geometry, usually ignoring hydrogen atoms, and taking account of multipole moments. In most cases, a simple model for dispersion forces and a multipole expansion taken at the first or first and second nonvanishing moments was enough. Hydrogen-bonded liquids are an exception, probably because we should consider more anisotropic forces than only those corresponding to molecular shape. In any case, the results are also fair for these kinds of liquids. Fitted dipole moments are consistently greater than experimental ones, usually obtained in the gaseous phase. This difference can be attributed to the additional induced dipole moment caused by the molecular polarizability of neighboring molecules in the liquid state. Consideration of the usual technical parameters also enabled us to examine important binary mixtures and to predict their miscibility at 293.15 K as an example. Ternary and more complex mixtures are very important, but a large amount of experimental information is necessary to give an idea of their phase diagram.[47] Solubility factors are usually the key to discussing their behavior, and thus, qualitatively important predictions could be made for a required mixture using only the results presented here. In this case, simulation is not only a factor making the process more straightforward but is also much cheaper for choosing regions where experiments would still be required.

**Acknowledgment.** This work was partially supported by Project PB94-0285 of the Spanish DGICYT and by Contract CI1*-CT94-0132 of the European Community. One of us (S.C.) expresses her gratitude for a grant from the Autonomous Community of Madrid to prepare her doctoral work.

## References and Notes

(1) Reid, R. C.; Prausnitz, J. M.; Poling, B. E. *The Properties of Gases and Liquids*, 4th ed.; McGraw-Hill: Singapore, 1988.
(2) Mühlbauer, A. L.; Raal, J. D. *Chem. Eng. J.* **1995**, *60*, 1. Sandler, S. I. In *Supercritical Fluids. Fundamentals for Application*; Kiran, E., Levelt Sengers, J. M. H., Eds.; NATO ASI Series E 273; Kluwer: Dordrecht, 1994.
(3) Vega, C.; Lago, S.; Padilla, P. *J. Phys. Chem.* **1992**, *96*, 1900.
(4) Vega, C.; Lago, S.; Pospisil, R.; Labik, S.; Malijevsky, A. *J. Phys. Chem.* **1992**, *96*, 1895.
(5) Lago, S.; López-Martín, J. L.; Garzón, B.; Vega, C. *J. Phys. Chem.* **1994**, *98*, 5355.
(6) Chapman, W. G.; Gubbins, K. E.; Jackson, G.; Radosz, M. *Fluid Phase Equilib.* **1989**, *52*, 31.
(7) Chapman, W. G.; Gubbins, K. E.; Radosz, M.; Jackson, G. *Ind. Eng. Chem. Res.* **1990**, *29*, 1709.
(8) Gil-Villegas, A.; Galindo, A.; Whitehead, P. J.; Mills, S. J.; Jackson, G.; Burgess, A. N. *J. Chem. Phys.* **1997**, *106*, 4168.
(9) Wertheim, M. S. *J. Stat. Phys.* **1984**, *35*, 19.
(10) Wertheim, M. S. *J. Stat. Phys.* **1984**, *35*, 35.
(11) Wertheim, M. S. *J. Stat. Phys.* **1986**, *42*, 459.
(12) Wertheim, M. S. *J. Stat. Phys.* **1986**, *42*, 477.
(13) Wertheim, M. S. *J. Chem. Phys.* **1986**, *85*, 2929.
(14) Wertheim, M. S. *J. Chem. Phys.* **1987**, *87*, 7323.
(15) Huang, S. H.; Radosz, M. *Ind. Eng. Chem. Res.* **1991**, *29*, 2284.
(16) Huang, S. H.; Radosz, M. *Ind. Eng. Chem. Res.* **1991**, *30*, 1994.
(17) Allen, M. P.; Tildesley, D. J. *Computer Simulation of Liquids*; Clarendon Press: Oxford, 1987.
(18) Vega, C.; Lago, S.; de Miguel, E.; Rull, L. F. *J. Phys. Chem.* **1992**, *96*, 7431.
(19) Garzón, B.; Lago, S.; Vega, C.; Rull, L. F. *J. Chem. Phys.* **1995**, *102*, 7204.
(20) Garzón, B.; Lago, S.; Vega, C.; de Miguel, E.; Rull, L. F. *J. Chem. Phys.* **1994**, *101*, 4166.
(21) Panagiotopoulos, A. Z. *Mol. Phys.* **1987**, *93*, 343.
(22) Kihara, T. *J. Phys. Soc. Jpn.* **1951**, *16*, 289.
(23) Siepmann, J. I.; Karaborni, S.; Smit, B. *J. Am. Chem. Soc.* **1993**, *115*, 6454.
(24) Smit, B.; Karaborni, S.; Siepmann, J. I. *J. Chem. Phys.* **1995**, *102*, 2126.
(25) van Leeuwen, M. E.; Smit, B. *J. Phys. Chem.* **1995**, *99*, 1831.
(26) van Leeuwen, M. E. *Mol. Phys.* **1996**, *87*, 87.
(27) Sevilla, P.; Lago, S. *Comput. Chem.* **1985**, *9*, 39.
(28) S. Lago and Vega, C. *Comput.Chem.* **1988**, *12*, 343.
(29) Vega, C.; Lago, S. *Comput. Chem.* **1994**, *18*, 55.
(30) Balescu, R. *Equilibrium and Nonequilibrium Statistical Mechanics*; Wiley: New York, 1975.
(31) Padilla, P.; Lago, S. *Fluid Phase Equilib.* **1989**, *48*, 53.
(32) Callen, H. B. *Thermodynamics and an Introduction to Thermostatistics*, 2nd ed.; Wiley: New York, 1985.
(33) Enciso, E.; Lado, F.; Lombardero, M.; Abascal, J. L. F.; Lago, S. *J. Chem. Phys.* **1987**, *87*, 2249.
(34) Smith, B. F.; Srisvastava, R. *Thermodynamic data for pure compounds. B. Halogenated Hydrocarbons and Alcohols*; Physical Sciences Data 25; Elsevier: Amsterdam, 1986.
(35) Widiatmo, J. V.; Sato, H.; Watanabe, K. *J. Chem. Eng. Data* **1994**, *39*, 404.
(36) Chao, J.; Gadalla, N. A. M.; Gammon, B. E.; Marsh, K. N.; Rodgers, A. S.; Somayajulu, G. R.; Wilhoit, R. C. *J. Phys. Chem. Ref. Data* **1990**, *19*, 1547.
(37) Kriebel, C.; Winkelmann, J. *Mol. Phys.* **1997**, *90*, 297.
(38) Armstrong, B. *J. Chem. Eng. Data* **1981**, *26*, 168.
(39) Stewart, R. B.; Jacobsen, R. T.; Wagner, W. *J. Phys. Chem. Ref. Data* **1991**, *20*, 917.
(40) Jacobsen, R. T.; Stewart, R. B. *J. Phys. Chem. Ref. Data* **1973**, *2*, 757.
(41) Younglove, B. A.; Ely, J. F. *J. Phys. Chem. Ref. Data* **1987**, *16*, 577.
(42) Calero, S.; Garzón, B.; MacDowell, L. G.; Lago, S. *J. Chem. Phys.* **1997**, *107*, 2034.
(43) Sato, H.; Uematsu, M.; Watanabe, K.; Okada, M. *Fluid Phase Equilib.* **1987**, *36*, 187.
(44) Mousa, A. H. N. *J. Chem. Thermodyn.* **1981**, *13*, 201. Warowny, W. *J. Chem. Eng.* **1994**, *39*, 275.
(45) Vega, C.; Garzón, B.; MacDowell, L. G.; Lago, S. *Mol. Phys.* **1995**, *85*, 679.
(46) Pitzer, K. S.; Lippmann, D. Z.; Curl, R. F.; Huggins, C. M.; Peterson, D. E. *J. Am. Chem. Soc.* **1955**, *77*, 3433.
(47) McHugh, M.; Krukonis, V. *Supercritical fluid extraction*; Butterworth-Heinemann: Stoneham, MA, 1994.
(48) Garzón, B.; Lago, S.; Vega, C. *Chem. Phys. Lett.* **1994**, *231*, 366.
(49) Gordon, H.; Goldman, S. *Mol. Simul.* **1989**, *2*, 177.
(50) *Handbook of Chemistry and Physics*, 67 ed.; Weast, R. C., Ed.; CRC Press: Boca Raton, FL, 1986.
(51) Drury, J. S. *Ind. Eng. Chem.* **1952**, *44*, 11.
(52) Moser, B.; Kistenmacher, H. *Fluid Phase Equilib.* **1987**, *34*, 189.